**Mathematical Modelling and Numerical Analysis** Will be set by the publisher
Modélisation Mathématique et Analyse Numérique

Sandia National Labs SAND2009-0115J

# SPECIAL FINITE ELEMENT METHODS BASED ON COMPONENT MODE SYNTHESIS TECHNIQUES

U. L. Hetmaniuk[1] and R. B. Lehoucq[2]

**Abstract**. The goal of our paper is to introduce a new approach for defining special finite element methods. Special finite elements denote methods of finite element type that employ special shape functions that, for instance, incorporate specialized knowledge about the governing equation. Our approach relies on the classic idea of component mode synthesis methods and exploits an orthogonal decomposition of the trial subspace to minimize the energy. Combining this space decomposition with a local eigendecomposition results in a systematic procedure to define special finite element methods. Numerical experiments illustrate the effectiveness of our new special finite element method.

**1991 Mathematics Subject Classification.** 35J20, 65F15, 65N25, 65N30, 65N55.

2 December 2008.

## 1. Introduction

The finite element solution of

$$\begin{cases} -\nabla \cdot c(x)\nabla u(x) = f(x) & \text{in } \Omega, \\ u(x) = 0 & \text{on } \partial\Omega, \end{cases} \tag{1}$$

has been the subject of much research (see [1,10,11] for overviews and references to the literature). The difficulty arises when the coefficient $c$ is composed of a multitude of spatial scales so that a naive application of the finite element method necessitates a highly refined mesh. Multiscale finite element methods incorporate the multiscale character of the coefficient $c$ so that fine-scale information is computed in an expedient manner. The underlying goal, then, is to first define an appropriate approximation space that has knowledge of the coefficient $c$, followed by an adroit choice of basis functions, for example functions of local support. These functions give rise to an effective finite element method when the method leads to a reasonably implemented algorithm with acceptable performance and sufficient accuracy. Babuška, Caloz, and Osborn [1, p. 947] denote such finite element methods *special*—an alternate distinction to multiscale that we use in this paper.

The goal of our paper is to provide a systematic procedure for determining an approximation space of functions for the numerical solution of (1). In contrast to other approaches, we exploit the fact that the solution $u$ of (1)

*Keywords and phrases:* eigenvalues, modal analysis, multilevel, substructuring, domain decomposition, dimensional reduction, finite elements

[1] Department of Applied Maths, University of Washington,Box 352420, Seattle, WA 98195-2420, (hetmaniu@u.washington.edu)

[2] Sandia National Laboratories, P.O. Box 5800, MS 1320, Albuquerque, NM 87185-1320 (rblehou@sandia.gov). Sandia is a multiprogram laboratory operated by Sandia Corporation, a Lockheed Martin Company, for the U.S. Department of Energy under contract DE-AC04-94AL85000.

© EDP Sciences, SMAI 1999

solves the minimization problem

$$\arg \min_{v \in H_0^1(\Omega)} \left( \frac{1}{2} \int_\Omega c(x) |\nabla v(x)|^2 \, dx - \int_\Omega f(x) v(x) \, dx \right) \tag{2}$$

and therefore is the minimum energy solution. This energy principle represents an intrinsic metric for comparing the quality of approximations to the solution of (1). Our procedure is based upon the classic idea of component mode synthesis (CMS), introduced in [5,9], and so solves the optimality system associated with (2) on a partition of the domain $\Omega$. Our approach is abstract and is not restricted to (1), e.g. elastostatics can also be considered.

### 1.1. Notation and Assumptions

We quickly review our use of standard notation. Let $\Omega$ be a two- or three-dimensional domain with Lipschitz boundary $\partial\Omega$ and so let $H^1(\Omega)$ denote a Sobolev space of order 1; let $H_0^1(\Omega)$ denote a subspace of $H^1(\Omega)$ consisting of functions that vanish on $\partial\Omega$. Let the norm and inner product on $H^1(\Omega)$ and $L^2(\Omega)$ be given by $\|\cdot\|_1, (\cdot,\cdot)_1$, and $\|\cdot\|, (\cdot,\cdot)$, respectively. Let

$$a(u,v) = \int_\Omega c(x) \nabla u(x) \cdot \nabla v(x) dx, \tag{3}$$

denote the bilinear form induced by (1). We suppose that $a(\cdot,\cdot)$ is coercive,

$$\exists \ \alpha > 0, \ 0 < \alpha \|v\|_1^2 \leq a(v,v), \quad \forall \ v \in H_0^1(\Omega), \tag{4}$$

and continuous,

$$\exists \ \gamma > 0, \ a(v,w) \leq \gamma \|v\|_1 \, \|w\|_1 \quad \forall \ v, w \in H_0^1(\Omega). \tag{5}$$

We rewrite (2) as

$$\arg \min_{v \in H_0^1(\Omega)} \left( \frac{1}{2} a(v,v) - (f,v) \right), \tag{6}$$

and the associated optimality system is the variational formulation of (1), e.g. given $f \in L^2(\Omega)$, find $u \in H_0^1(\Omega)$ such that

$$a(u,v) = (f,v) \quad \forall v \in H_0^1(\Omega). \tag{7}$$

We refer to the solutions of (1), (2), and (7) as equivalent in a formal sense.

## 2. Eigen decomposition

The minimization problem (2) explains that the natural approximation space is that generated by the eigenmodes for the associated variational problem: Find $(z_*, \lambda_*) \in H_0^1(\Omega) \times \mathbb{R}$ such that

$$a(z_*, v) = \lambda_* \, (z_*, v) \quad \forall v \in H_0^1(\Omega). \tag{8}$$

We will refer to (8) as the global eigenvalue problem. Straightforward arguments show the eigenvalues are positive and the eigenvectors are orthogonal with respect to the inner product induced by $a(\cdot,\cdot)$ and the $L^2$ inner product. We assume that the eigenvalues $\{\lambda_i\}_{i=1}^\infty$ are ordered into a nondecreasing sequence and that the eigenmodes $z_i$ are normalized for the $L^2$ inner product, *i.e.* $(z_i, z_i) = 1$.

The source term $f$ and the solution $u$ of (2) have the expansions

$$f = \sum_{i=1}^\infty (f, z_i) z_i \quad \text{and} \quad u = \sum_{i=1}^\infty \frac{(f, z_i)}{\lambda_i} z_i. \tag{9}$$

Sandia National Labs SAND2009-0115J

Sandia National Labs SAND2009-0115J

We define the finite-dimensional subspace

$$V_{EIG} = \text{span}\{z_i; 1 \leq i \leq I\}. \tag{10}$$

The approximate solution $u_{EIG}$ satisfies

$$a(u_{EIG}, v) = (f, v) \quad \forall v \in V_{EIG}, \tag{11}$$

and is given by the truncated series

$$u_{EIG} = \sum_{i=1}^{I} \frac{(f, z_i)}{\lambda_i} z_i. \tag{12}$$

The following two estimates easily follow

$$a\left(u - \sum_{i=1}^{I} \frac{(f, z_i)}{\lambda_i} z_i, u - \sum_{i=1}^{I} \frac{(f, z_i)}{\lambda_i} z_i\right) \leq \frac{1}{\lambda_{I+1}} \| \sum_{i=I+1}^{\infty} (f, z_i) z_i \|^2 \tag{13a}$$

$$\| u - \sum_{i=1}^{I} \frac{(f, z_i)}{\lambda_i} z_i \|^2 \leq \frac{1}{\lambda_{I+1}^2} \| \sum_{i=I+1}^{\infty} (f, z_i) z_i \|^2. \tag{13b}$$

Hence, a good approximation by the low-energy eigenmodes requires that the high-frequency components of $f$ normalized by the first unused eigenvalue are negligible. In principal, knowledge of the eigenmodes provides a finite-dimensional subspace that allows many problems (7) to be solved efficiently. Unfortunately, the eigenmodes have global support and computing them results in a nontrivial computation.

## 3. Component mode synthesis

We review the classical technique of component mode synthesis [5,9] from an abstract perspective. Partition the domain $\Omega$ into $J$ non intersecting subdomains $\Omega_j, j = 1, \cdots, J$, that share the common interface $\Gamma$; see Figure 1 for the case of 4 subdomains.

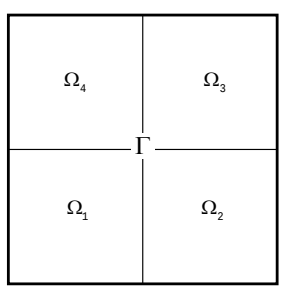


Figure 1. The domain $\Omega$ partitioned four subdomains.

Let $V_{\Omega_j}$ be the subspace of local functions that are nonzero in $\Omega_j$ and are trivially extended throughout $\Omega$,

$$V_{\Omega_j} = \{v \in H_0^1(\Omega) \colon v|_{\Omega \setminus \Omega_j} = 0\}. \tag{14}$$

We remark that any member function of $V_{\Omega_j}$ has a zero trace on the boundary $\partial\Omega$ and on the interface $\Gamma$. Let $V_\Gamma$ be the subspace of harmonic extensions of trace functions on $\Gamma$,

$$V_\Gamma = \{E_\Omega \tau \in H_0^1(\Omega) \colon \tau \in H_{00}^{1/2}(\Gamma)\}, \tag{15}$$

where $H_{00}^{1/2}(\Gamma)$ denotes the trace space of $H_0^1(\Omega)$ on $\Gamma$ and the harmonic extension $E_\Omega$ of $\tau \in H_{00}^{1/2}(\Gamma)$ solves the minimization problem

$$\inf_{v \in H_0^1(\Omega)} a(v,v) \quad \text{subject to} \quad v|_\Gamma = \tau.$$

We remark that the harmonic extension $E_\Omega$ satisfies also

$$\left\{ \begin{array}{rcll} -\nabla \cdot c(x) \nabla E_\Omega \tau(x) & = & 0 & \text{in } \Omega_j, \text{ for all } j, \\ E_\Omega \tau & = & \tau & \text{on } \Gamma, \\ E_\Omega \tau & = & 0 & \text{on } \partial\Omega. \end{array} \right. \tag{16}$$

This property indicates that functions in $V_\Gamma$ are governed by the underlying partial differential equation. Note that any non-zero member function of $V_\Gamma$ has a non-zero trace on $\Gamma$. When the coefficient $c$ is composed of a multitude of spatial scales, members of $V_\Gamma$ carry fine-scale information among subdomains, while the members of $V_{\Omega_j}$ hold only fine-scale information within the subdomain $\Omega_j$.

The key result that enables our systematic process for deriving and comparing the quality of special finite element methods is the orthogonal decomposition

$$H_0^1(\Omega) = \left( \bigoplus_{j=1}^{J} V_{\Omega_j} \right) \oplus V_\Gamma. \tag{17}$$

Although not often stated in this form, this is a well-known result, at the heart of the analysis and development of domain decomposition methods for elliptic partial differential equations [12], and modern component mode synthesis methods [3,4] for the numerical solution of the global eigenvalue problem (8).

The decomposition (17) is orthogonal with respect to the inner product $a(\cdot,\cdot)$ because

$$a(v_i, v_j) = 0, \; \forall \; v_i \in V_{\Omega_i}, \; \forall \; v_j \in V_{\Omega_j}, \; (i \neq j), \tag{18a}$$

$$a(v_i, v_\Gamma) = 0, \; \forall \; v_i \in V_{\Omega_i}, \; \forall \; v_\Gamma \in V_\Gamma. \tag{18b}$$

The decomposition (17) implies also that

$$\min_{v \in H_0^1(\Omega)} \left( \frac{1}{2} a(v,v) - (f,v) \right) = \sum_{j=1}^{J} \min_{v \in V_{\Omega_j}} \left( \frac{1}{2} a(v,v) - (f,v) \right) + \min_{v \in V_\Gamma} \left( \frac{1}{2} a(v,v) - (f,v) \right) \tag{19}$$

and that the solution of (7) is the sum of $J$ local functions, respectively in $V_{\Omega_1}, \cdots, V_{\Omega_J}$, and a function of $V_\Gamma$, *i.e.*

$$u = u_1 + \cdots + u_J + u_\Gamma \tag{20}$$

where $u_j$ and $u_\Gamma$ minimizes the energy in $V_{\Omega_j}$ and $V_\Gamma$, respectively. The local solutions $u_j \in V_{\Omega_j}$ and $u_\Gamma \in V_\Gamma$ are also the orthogonal projections of the solution $u$ for (7) onto the respective subspaces. The orthogonal decomposition of the solution given by (20) explains that the purpose of $u_\Gamma \in V_\Gamma$ is to couple the $J$ subdomain solutions $u_j$. Component mode synthesis is thus defined where components from the $J+1$ subspaces are synthesized to approximate a global function.

A natural approximating subspace consistent with the decomposition (17) arises from selecting a subset of eigenmodes for $a(\cdot,\cdot)$ in the subspaces $V_{\Omega_j}$ and $V_\Gamma$. We define $J$ *fixed-interface* eigenvalue problems: Find $(z_{*,j}, \lambda_{*,j}) \in V_{\Omega_j} \times \mathbb{R}$ such that

$$a(z_{*,j}, v) = \lambda_{*,j} \, (z_{*,j}, v) \quad \forall v \in V_{\Omega_j}, \tag{21}$$

Sandia National Labs SAND2009-0115J

and the *coupling* eigenvalue problem: Find $(z_{*,\Gamma}, \lambda_{*,\Gamma}) \in V_\Gamma \times \mathbb{R}$ such that

$$a(z_{*,\Gamma}, v) = \lambda_{*,\Gamma}(z_{*,\Gamma}, v) \quad \forall v \in V_\Gamma. \tag{22}$$

Note that the only differences between these two eigenvalue problems are the approximating spaces $V_{\Omega_j}$ and $V_\Gamma$. We assume that the eigenvalues $\{\lambda_{i,j}\}_{i=1}^\infty$ and $\{\lambda_{i,\Gamma}\}_{i=1}^\infty$ are ordered into nondecreasing sequences and that the eigenmodes $z_{*,j}$ and $z_{*,\Gamma}$ are normalized for the $L^2$ inner product.

The fixed-interface and coupling eigenmodes can then be employed to expand the source term $f$ and the solution $u$ of (2)

$$f = \sum_{j=1}^J \sum_{i=1}^\infty (f, z_{i,j}) z_{i,j} + \sum_{i=1}^\infty (f, z_{i,\Gamma}) z_{i,\Gamma} \quad \text{and} \quad u = \sum_{j=1}^J \sum_{i=1}^\infty \frac{(f, z_{i,j})}{\lambda_{i,j}} z_{i,j} + \sum_{i=1}^\infty \frac{(f, z_{i,\Gamma})}{\lambda_{i,\Gamma}} z_{i,\Gamma}. \tag{23}$$

We define the finite-dimensional subspace

$$V_{CMS} = \left( \bigoplus_{j=1}^J \text{span}\{z_{i,j}; 1 \le i \le I_j\} \right) \oplus \text{span}\{z_{i,\Gamma}; 1 \le i \le I_\Gamma\}, \tag{24}$$

where $I_j$ and $I_\Gamma$ are non-negative integers. The approximate solution $u_{CMS}$ satisfies

$$a(u_{CMS}, v) = (f, v), \quad \forall v \in V_{CMS}, \tag{25}$$

and is given by the truncated series

$$u_{CMS} = \sum_{j=1}^J \sum_{i=1}^{I_j} \frac{(f, z_{i,j})}{\lambda_{i,j}} z_{i,j} + \sum_{i=1}^{I_\Gamma} \frac{(f, z_{i,\Gamma})}{\lambda_{i,\Gamma}} z_{i,\Gamma}. \tag{26}$$

The following energy estimate easily follows

$$a(u - u_{CMS}, u - u_{CMS}) \le \sum_{j=1}^J \frac{1}{\lambda_{I_j+1,j}} \| \sum_{i=I_j+1,j}^\infty (f, z_{i,j}) z_{i,j} \|^2 + \frac{1}{\lambda_{I_\Gamma+1,\Gamma}} \| \sum_{i=I_\Gamma+1,\Gamma}^\infty (f, z_{i,\Gamma}) z_{i,\Gamma} \|^2 \tag{27}$$

and a similar estimate holds for the $L^2$ norm. This energy estimate indicates that an accurate approximation of $u$ is obtained when fixed-interface eigenmodes and coupling modes are combined in the approximation subspace. On the other hand, when the approximation subspace does not contain any fixed-interface mode, the energy norm of the error becomes

$$a(u - u_{CMS}, u - u_{CMS}) = \sum_{j=1}^J a(u_j, u_j) + \sum_{i=I_\Gamma+1,\Gamma}^\infty \frac{(f, z_{i,\Gamma})^2}{\lambda_{i,\Gamma}} \tag{28}$$

Unless all the local solutions $u_j \in V_{\Omega_j}$ are zero, the error $u - u_{CMS}$ can not converge to zero as $I_\Gamma \to \infty$ when the approximation subspace does not contain any fixed-interface mode. A similar remark holds when the approximation subspace does not contain any coupling modes.

By introducing $J$ subdomains, the cost of computing eigenmodes in $V_{\Omega_j}$ decreases over that of computing eigenmodes in $H_0^1(\Omega)$ and so becomes tractable. Hence, subsets of eigenmodes in $V_{\Omega_j}$ can be used to define an approximating space of $H_0^1(\Omega)$. Unfortunately, the cost of approximating eigenmodes associated with the coupling mode problem remains daunting because a generalized eigenvalue problem composed of Schur and mass complement operators is a nontrivial computation; see the survey paper [6] for details. We are thus motivated

Sandia National Labs SAND2009-0115J

to consider variants of component mode synthesis for deriving local approximations to the coupling eigenmodes, or members of $V_\Gamma$.

## 4. New special finite element method

Numerous choices of basis functions are possible for defining a discrete subspace of $H_0^1(\Omega)$. No general basis exists to solve problem (1) robustly for any coefficient $c$. An exception is Laplace's equation (e.g. $c = 1$) where the nodal Lagrangian finite element method leads to a robust general method. However, when the coefficient $c$ is composed of a multitude of spatial scales, the classical Lagrangian finite element method necessitates a highly refined mesh to compute an accurate solution. Indeed, the mesh should be refined well enough to capture all the features of $c$ so that, per element, the problem is well approximated by Laplace's equation.

One would like to find a finite-dimensional approximation subspace of $H_0^1(\Omega)$ that performs almost as well as the space generated by the lowest frequency eigenmodes without the ensuing cost of computation. Babuška, Caloz, and Osborn [1] use the phrase special finite elements to denote methods of finite element type that employ special shape functions that, for instance, incorporate specialized knowledge of the partial differential operator. We use the same terminology. Using the global eigenmodes as special shape functions incorporates information about the partial differential operator. Many methods have been proposed to incorporate relevant information into the special shape functions (see [1, 2, 7, 10, 11, 13] and the references therein). For example, Nolen, Papanicolaou, and Pironneau [11] exploits the variational multiscale framework [8] to define special shape functions. In this paper, we choose to exploit the decomposition (17) for incorporating information about the partial differential equation and its coefficient. We propose to select basis functions from the subspaces $V_{\Omega_j}$ and $V_\Gamma$ that satisfy the constraint of local support.

To simplify the presentation, we assume that $\Omega = (0, 1) \times (0, 1)$. Let $\mathcal{T}$ be a partition of $\Omega$ into rectangles $K_j$. The subdomains $\Omega_j$ are set to be equal to the rectangles $K_j$. The interface $\Gamma$ is the union of all the interior edges between two rectangles. We remind the reader that the subspace $V_{\Omega_j}$, defined by (14), contain functions of zero trace on $\Gamma$ and can only hold information on the subdomain $\Omega_j$. Functions of $V_\Gamma$ (15) are governed by the underlying partial differential equation because they are harmonic extensions in $\Omega$ of trace functions on $\Gamma$. They satisfy the boundary value problem (16).

The discretization space that we are proposing is consistent with the decomposition (17) and all the basis functions have local support. We define the subspace

$$V_{ACMS} = \left( \bigoplus_{j=1}^{J} \text{span}\{z_{1,j}\} \right) \oplus \left[ \left( \bigoplus_{P \in \mathcal{T}_c} \text{span}\{\phi_P\} \right) \oplus \left( \bigoplus_{P \in \mathcal{T}_c} \text{span}\{\psi_{P,1}, \psi_{P,2}, \psi_{P,3}, \psi_{P,4}\} \right) \right] \tag{29}$$

where $z_{1,j}$ is the first *fixed-interface* mode (21) in $\Omega_j$ and the letter $A$ in $ACMS$ stands for approximate.

For any interior point $P$ of the partition $\mathcal{T}$, $\phi_P$ belongs to $V_\Gamma$ and is a harmonic extension satisfying

$$\begin{cases} -\nabla \cdot c(x) \nabla \phi_P(x) &= 0 \quad \text{in } \Omega_j, \\ \phi_P &\neq 0 \quad \text{on } \Gamma \end{cases} \tag{30}$$

for any subdomain $\Omega_j$. The trace of $\phi_P$ on $\Gamma$ is a piecewise-linear function such that $\phi_P(P) = 1$ and $\phi_P$ is zero at all the other nodes (see Figure 2 for a plot of the trace of $\phi_P$). The support of $\phi_P$ consists of the elements sharing the point $P$ and is local. This special shape function was used in the MFEM-L approach of Hou and Wu [7, Section 2.2] and in the residual free bubble method of Sangalli [13, Section 2.2].

The function $\psi_{P,i}$ belongs also to $V_\Gamma$ and is the harmonic extension of $\tau_{P,i} \in H_{00}^{1/2}(\Gamma)$, whose support is an edge, $\Sigma_{P,i}$, between two elements sharing $P$. The trace function $\tau_{P,i}$ is the first eigenmode for the *coupling* mode problem:

$$a(E_\Omega \tau_{P,I}, E_\Omega \eta) = \lambda (E_\Omega \tau_{P,I}, E_\Omega \eta), \quad \forall\, \eta \in H_{00}^{1/2}(\Gamma) \text{ such that } \text{supp}(\eta) \subset \Sigma_{P,i}. \tag{31}$$

Sandia National Labs SAND2009-0115J

Sandia National Labs SAND2009-0115J

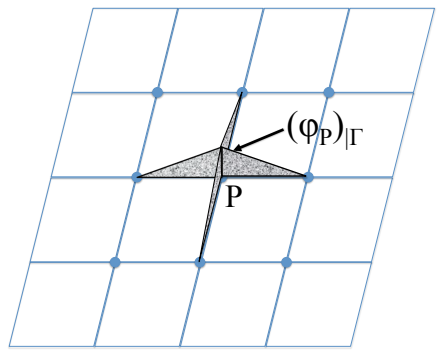


FIGURE 2. Trace of $\phi_P$ along $\Gamma$ for a domain partitioned into 16 subdomains

An example for $\tau_{P,3} = (\psi_{P,3})_{|\Gamma}$ is given in Figure 3.

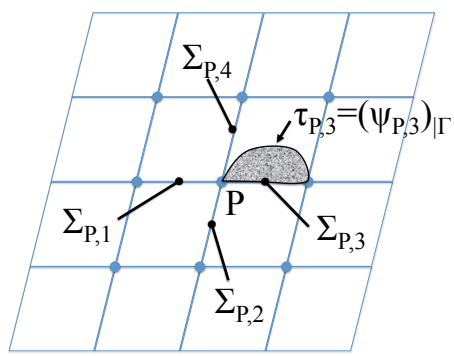


FIGURE 3. Example of a local coupling mode around a point $P$.

The finite-dimensional approximation subspace $V_{ACMS}$ is a special finite element method. This subspace exploits the orthogonal decomposition (17) for incorporating information about the variational form $a(\cdot,\cdot)$. The subspace $V_{ACMS}$ contains information within a subdomain $\Omega_j$ via the first fixed-interface mode. The functions $\phi_P$ carry information among four subdomains and $\psi_{P,i}$ between two subdomains. All these special shape functions have local support. The generalization of $V_{ACMS}$ to triangular cells is straightforward. The special shape functions $z_{1,j}$, $\phi_P$, and $\psi_{P,i}$ are computed via a finite element discretization within each element $K$. Further details are given in Section 5. Before presenting the numerical experiments, we discuss other choices of finite-dimensional approximation subspaces.

The standard nodal linear finite element method (Q1) defines an approximation subspace $V_{Q1}$

$$V_{Q1} = \text{span}\,\{N_P;\ P \in \mathcal{T}\} \tag{32}$$

where $N_P$ is the bilinear nodal shape function for an interior point $P$. When $c$ is a constant, for any interior point $P$, the associated nodal shape function $N_P$ belongs to $V_\Gamma$ because $N_P$ satisfies

$$\begin{cases} -\nabla \cdot c(x)\nabla N_P &= 0 \quad \text{in } \Omega_j, \text{ for all } j, \\ N_P &\neq 0 \quad \text{on } \Gamma, \\ N_P &= 0 \quad \text{on } \partial\Omega. \end{cases} \tag{33}$$

Therefore, when $c$ is a constant, $V_{Q1}$ is a finite-dimensional subspace of $V_\Gamma$ that does not have any component in the subspaces $V_{\Omega_j}$.

However, when $c$ is varying, the approximation subspace $V_{Q1}$ is no longer a subspace of $V_\Gamma$. For any interior point $P$, the nodal shape function $N_P$ is not a member of $V_\Gamma$ because $N_P$ is no longer an harmonic extension, *i.e.*

$$\nabla \cdot c(x)\nabla N_p \neq 0 \quad \text{in } \Omega_j, \tag{34}$$

when $\Omega_j$ intersects the support of $N_P$. The nodal shape function $N_P$ is not a member of $\Omega_j$ either because its trace on $\Gamma$ is non zero. Therefore the nodal shape function $N_P$ has nonzero components in $V_\Gamma$ and some $V_{\Omega_j}$ in stark contrast to $\phi_P$ defined by (30).

The MFEM-L approach of Hou and Wu [7] selects basis functions exclusively from $V_\Gamma$. This approach relies on the following subspace

$$V_{MFEM-L} = \left( \bigoplus_{P \in \mathcal{T}} \text{span}\{\phi_P\} \right) \subset V_\Gamma \subset H_0^1(\Omega) \tag{35}$$

where $\phi_P$ is the same harmonic extension used in $V_{ACMS}$ (see (30)). When $c$ is constant, MFEM-L is equivalent to the linear finite element method, $V_{MFEM-L} = V_{Q1}$. When $c$ is varying, $V_{MFEM-L}$ remains a subspace of $V_\Gamma$ and differs from $V_{Q1}$. From the point view of decomposition (17), MFEM-L is a generalization of the linear finite element method for a varying coefficient $c$ that retains the property $V_{MFEM-L} \subset V_\Gamma$. As remarked, the MFEM-L approach does not have any component in the subspaces $V_{\Omega_j}$. So the error formula (28) implies that the energy of the local solutions $u_j$ may limit the accuracy of the approximate solution computed in $V_{MFEM-L}$.

## 5. Numerical Experiments

### 5.1. Computation of basis functions

We will solve problems in $\Omega = (0,1) \times (0,1)$. Let $\mathcal{T}_n$ be a partition of $\Omega$ with $n$ square elements per direction and a uniform mesh size $h = 1/n$. To compute the special shape functions $z_{1,*}$, $\phi_P$, and $\psi_{P,*}$, each element is divided into $m \times m$ square elements with $h_f = h/m$.

We use piecewise bilinear elements to compute the special shape functions. The assembly of the stiffness matrix and the right-hand side vector requires the computation of volume integrals

$$\int_{K=\Omega_j} c(x)\nabla\phi_P(x) \cdot \nabla\psi_{P,1}(x)dx \tag{36}$$

on $\mathcal{T}_h$. We exploit the expression of $\phi_P$ and $\psi_{P,1}$ on the submesh contained in $K = \Omega_j$

$$\phi_P = \sum_{P_f \in K} \chi_{P_f} N_{P_f} \quad \text{and} \quad \psi_P = \sum_{P_f \in K} \xi_{P_f} N_{P_f} \tag{37}$$

where $N_{P_f}$ is the piecewise bilinear shape function for the point $P_f$ on the submesh contained in $K$. Using the stiffness matrix $\mathbf{K}_f$ computed on the submesh, we write

$$\int_K c(x)\nabla\phi_P(x) \cdot \nabla\psi_{P,1}(x)dx = \left[(\chi_{P_f})_{P_f \in K}\right]^T \mathbf{K}_f \left[(\xi_{P_f})_{P_f \in K}\right] \tag{38}$$

Sandia National Labs SAND2009-0115J

The other volume integrals are computed similarly. To solve linear systems and eigenproblems, we use direct solvers from Matlab.

### 5.2. **Experiments with the Laplace equation**

Consider the problem

$$\left\{ \begin{array}{rcll} -\Delta u & = & f & \text{on } \Omega \\ u & = & 0 & \text{in } \partial\Omega \end{array} \right. \tag{39}$$

We choose $f(x,y) = 2x(1-x) + 2y(1-y)$ such that the exact solution $u$ is $x(1-x)y(1-y)$.

Introduce a mesh $\mathcal{T}_n$ composed of squares with uniform mesh size $h = 1/n$. $\mathcal{T}_n$ contains $n^2$ elements, $(n-1)^2$ interior points, and $2n(n-1)$ interior edges. We compare the accuracy of computed solutions when using different finite-dimensional subspaces.

Table 1 lists the dimensions for the different approximation subspaces. With bilinear finite elements, the

| Subspace | Dimension | Stencil Width |
|---|---|---|
| $V_{Q1}$ | $(n-1)^2$ | 9 |
| $V_{ACMS}$ | $(2n-1)^2$ | 21 |
| $V_{CMS}$ | $(2n-1)^2$ | 1 |
| $V_{EIG}$ | $(n-1)^2$ | 1 |

TABLE 1. Dimension and stencil width for different special finite element methods

subspace $V_{Q1}$ (32) has $(n-1)^2$ degrees of freedom. For our proposed special finite element method, the subspace $V_{ACMS}$ (29) has $n^2$ fixed interface modes, $(n-1)^2$ functions $\phi_P$, and $2n(n-1)$ edge functions. The dimension of $V_{ACMS}$ is

$$n^2 + (n-1)^2 + 2n(n-1) = (n+n-1)^2 = (2n-1)^2.$$

For the sake of comparison, we use also the subspace $V_{CMS}$ (24) with 1 fixed-interface mode per element and $(2n-1)^2 - n^2$ coupling modes. The dimension of $V_{CMS}$ is also $(2n-1)^2$. Finally, we compute the solution with $V_{EIG}$ when the first $(n-1)^2$ eigenmodes are used. We recall that, for the Laplace equation, that MFEM-L is equivalent to the bilinear finite element method. So, for this example, we do not use the MFEM-L approach.

Table 1 lists also the stencil width on a uniform mesh $\mathcal{T}_n$ or the maximum number of non-zero entries per row for the stiffness matrix. Note that, with $V_{EIG}$ and $V_{CMS}$, the resulting stiffness matrix is diagonal. With $V_{Q1}$, each row of the stiffness matrix has at most 9 non-zero entries. With $V_{ACMS}$, the stiffness matrix contains a diagonal block for the $n^2$ fixed interface modes. A row associated with $\phi_P$ (respectively $\psi_{P,i}$) has at most 21 (resp. 13) non-zero entries.

Figure 4 plots convergence curves for the $H^1$ semi-norm, which corresponds to the energy norm, in terms of the number of degrees of freedom. The number of degrees of freedom is, indeed, more relevant than the mesh size $h$ or the number of elements per direction $n$. As highlighted in Table 1, the considered approximation subspaces have different dimensions on the same mesh $\mathcal{T}_n$. As expected, the bilinear finite element has a convergence rate proportional to $h$ or to the square root of the total number of degrees of freedom. The curves for $V_{CMS}$ and $V_{ACMS}$ are indistinguishable, indicating that the basis functions in $V_{ACMS} \cap V_\Gamma$ with local support approximate well the subspace spanned by the global eigenmodes for the Schur and mass complements.

For a fixed number of degrees of freedom, the approximate solution computed in $V_{EIG}$ is the most accurate followed by the subspaces $V_{CMS}$ and $V_{ACMS}$. For this problem, the approximate solution in $V_{Q1}$ is the least accurate. To reach a fixed level of accuracy for this problem,

- $V_{EIG}$ requires 40 times less degrees of freedom than $V_{Q1}$,
- $V_{CMS}$ and $V_{ACMS}$ require 5 times less degrees of freedom than $V_{Q1}$.

For the curves in Figure 4, the special basis functions $z_{1,*}$, $\phi_P$, and $\psi_{P,*}$, were approximated with $16 \times 16$ bilinear finite elements in a square element of $\mathcal{T}_n$, *i.e.* $h_f = h/16$. Figure 5 illustrates the convergence of the

Sandia National Labs SAND2009-0115J

Sandia National Labs SAND2009-0115J

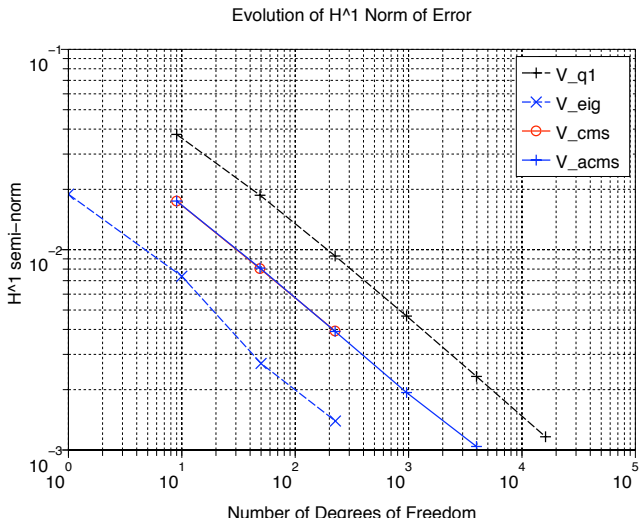


FIGURE 4. Comparison of special finite element methods for problem (39).

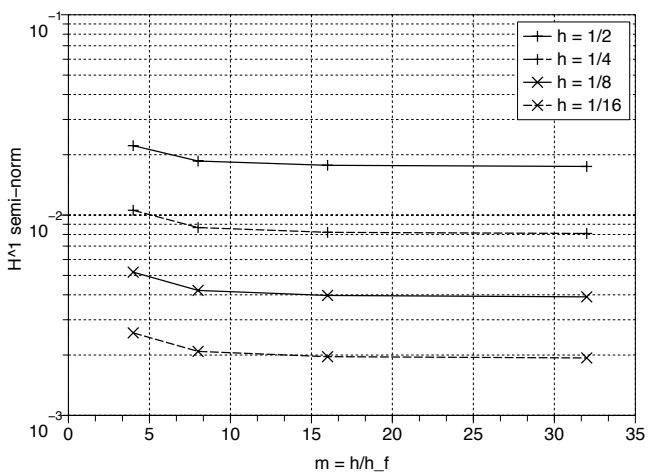


FIGURE 5. Effect of subcell mesh size to compute basis functions of $V_{ACMS}$ for problem (39).

$H^1$ semi-norm for the subspace $V_{ACMS}$ for a fixed mesh size $h$ as $m = h/h_f$ increases. A ratio of $m = 16$ is sufficient to compute numerically the special basis functions.

### 5.3. **Experiments with a varying coefficient**

Consider the problem

$$\left\{ \begin{array}{rcll} -\nabla \cdot \left( \dfrac{1}{1.2 + \cos(32\pi x(1-x)y(1-y))} \nabla u \right) & = & f & \text{on } \Omega \\ u & = & 0 & \text{in } \partial\Omega \end{array} \right. \tag{40}$$

We choose $f(x,y) = 64\pi\,[x(1-x) + 2y(1-y)]$ such that the exact solution $u$ is

$$u(x,y) = (1.2 \times 32\pi)x(1-x)y(1-y) + \sin(32\pi x(1-x)y(1-y)).$$

Note that the coefficient $c$ oscillates while the source term $f$ does not.

Introduce a mesh $\mathcal{T}_n$ composed of squares with uniform mesh size $h = 1/n$. $\mathcal{T}_n$ contains $n^2$ elements, $(n-1)^2$ interior points, and $2n(n-1)$ interior edges. We compare the accuracy of computed solutions when using the finite-dimensional subspaces $V_{Q1}$, $V_{MFEM-L}$, $V_{ACMS}$, $V_{CMS}$, and $V_{EIG}$. Since the coefficient $c$ is varying, the subspace $V_{MFEM-L}$ is different from the subspace $V_{Q1}$. The dimension of $V_{MFEM-L}$ is $(n-1)^2$ and the resulting stiffness matrix has at most 9 non-zero entries per row.

Figure 6 plots convergence curves for the energy norm of the error in terms of the number of degrees of freedom. For the curves in Figure 6, the special basis functions were approximated with, at least, $16 \times 16$

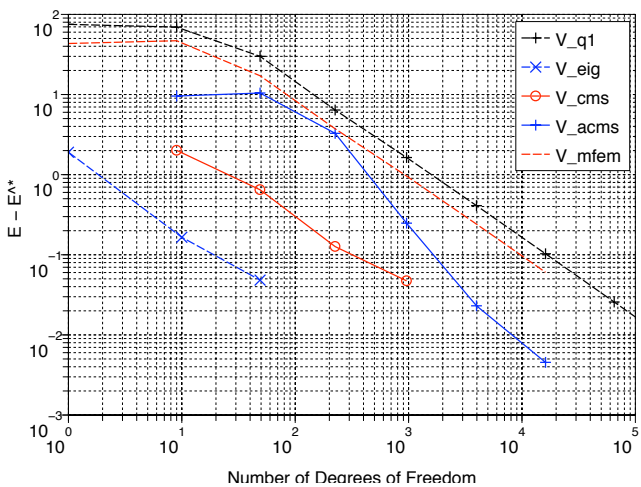


FIGURE 6. Comparison of special finite element methods for problem (40).

bilinear finite elements in any square element of $\mathcal{T}_n$, *i.e.* $h_f \le h/16$.

The energy norm is computed by subtracting the energy of the computed solution from the energy of the exact solution $u$. Indeed, we have

$$\left(\frac{1}{2}a(u_{Q1},u_{Q1}) - (f,u_{Q1})\right) - \left(\frac{1}{2}a(u,u) - (f,u)\right) = \frac{1}{2}a(u_{Q1},u_{Q1}) - (f,u_{Q1}) + \frac{1}{2}a(u,u) \tag{41a}$$

$$= \frac{1}{2}\left(a(u_{Q1},u_{Q1}) - 2(f,u_{Q1}) + a(u,u)\right) \tag{41b}$$

$$= \frac{a(u-u_{Q1},u-u_{Q1})}{2} \tag{41c}$$

when the approximate solution is $u_{Q1}$ and where we used

$$a(u,u_{Q1}) = (f,u_{Q1}) \quad \text{and} \quad a(u,u) = (f,u)$$

Sandia National Labs SAND2009-0115J

(from (7)). This difference of energy is an intrinsic metric for comparing the quality of approximations. When the exact solution $u$ is not explicitly known, approximating the minimal energy,

$$E^* = \frac{1}{2}a(u,u) - (f,u) = -\frac{a(u,u)}{2} = -\frac{(f,u)}{2}, \tag{42}$$

is simpler than extrapolating the exact solution.

As expected, the bilinear finite element has a convergence rate proportional to $h^2$ or to the total number of degrees of freedom. The approximation with $V_{ACMS}$ appears to require a finer mesh to reach the asymptotic regime. Before reaching its asymptotic regime, the curve for $V_{ACMS}$ exhibits a bump. Here, the curves for $V_{CMS}$ and $V_{ACMS}$ are different. But the curve for $V_{ACMS}$ appears to reach asymptotically tue curve for $V_{CMS}$, which would be consistent with the experiment for the Laplace equation. Further analysis is required to understand the asymptotic behaviors and to understand why the approximation with $V_{ACMS}$ lags that with $V_{MFEM-L}$ or $V_{Q1}$ for attaining the asymptotic regime.

To reach a fixed level of accuracy for this problem,

- $V_{MFEM-L}$ requires 2 times less degrees of freedom than $V_{Q1}$,
- $V_{ACMS}$ requires between 2 and 10 times less degrees of freedom than $V_{Q1}$,
- $V_{CMS}$ and $V_{EIG}$ require at least 50 times less degrees of freedom than $V_{Q1}$.

For a fixed number of degrees of freedom, the approximate solution computed in $V_{EIG}$ is the most accurate followed by the subspaces $V_{CMS}$, $V_{ACMS}$, $V_{MFEM-L}$. The approximate solution in $V_{Q1}$ is the least accurate. We recall that $V_{EIG}$ and $V_{CMS}$ are not practical because they demand a large number of global eigenmodes whose computations are daunting (and in fact prevented us from computing more data points in Figure 6 as the number of degrees of freedom increases).

## 6. Conclusions

We have presented a systematic approach to define special finite element methods. The approach is based on the classic idea of component mode synthesis and exploits a $H_0^1(\Omega)$ orthogonal decomposition. By using local eigenmodes of the solution, special finite element methods are defined. On academic examples, the new approximation subspace $V_{ACMS}$ is, for the same number of degrees of freedom, more accurate than the bilinear finite element.

## References

[1] I. Babuška, G. Caloz, and J. Osborn. Special finite element methods for a class of second order elliptic problems with rough coefficients. *SIAM J. Numer. Anal.*, 31(4):945–981, 1994.

[2] I. Babuška and J. E. Osborn. Generalized finite element methods: Their performance and their relation to mixed methods. *SIAM J. Numer. Anal.*, 20(3):510–536, 1983.

[3] J. K. Bennighof and R. B. Lehoucq. An automated multilevel substructuring method for eigenspace computation in linear elastodynamics. *SIAM J. Sci. Comput.*, 25(6):2084–2106, 2004.

[4] F. Bourquin. Component mode synthesis and eigenvalues of second order operators: Discretization and algorithm. *Mathematical Modelling and Numerical Analysis*, 26:385–423, 1992.

[5] R. R. Craig, Jr. and M. C. C. Bampton. Coupling of substructures for dynamic analysis. *AIAA Journal*, 6(7):1313–1319, 1968.

[6] U. Hetmaniuk and R. B. Lehoucq. Multilevel methods for eigenspace computations in structural dynamics. In *Domain Decomposition Methods in Science and Engineering*, volume 55 of *Lecture Notes in Computational Science and Engineering*, pages 103–114. Springer-Verlag, 2007.

[7] T. Hou and X. Wu. A multiscale finite element method for elliptic problems in composite materials and porous media. *J. Comput. Phys.*, 134:169–189, 1997.

[8] T. Hughes and G. Sangalli. Variational multiscale analysis: the fine-scale Green's function, projection, optimization, localization, and stabilized methods. *SIAM J. Numer. Anal.*, 45(2):539–557, 2007.

[9] W. C. Hurty. Vibrations of structural systems by component-mode synthesis. *Journal of the Engineering Mechanics Division, ASCE*, 86:51–69, 1960.

[10] P. Ming and X. Yue. Numerical methods for multiscale elliptic problems. *J. Comput. Phys.*, 214(1):421–445, 2006.

Sandia National Labs SAND2009-0115J

[11] J. Nolen, G. Papanicolaou, and O. Pironneau. A framework for adaptive multiscale methods for elliptic problems. *Multiscale Modeling & Simulation*, 7(1):171–196, 2008.

[12] A. Quarteroni and A. Valli. *Domain Decomposition Methods for Partial Differential Equations*. Numerical Mathematics and Scientific Computation. Oxford University Press, Oxford, UK, first edition, 1999.

[13] G. Sangalli. Capturing small scales in elliptic problems using a residual-free bubbles finite element method. *Multiscale Modeling & Simulation*, 1(3):485–503, 2003.

Sandia National Labs SAND2009-0115J